Revista Mexicana de Astronomía y Astrofísica, **53**, 67–78 (2017)

THE CHROMOSPHERICALLY ACTIVE LOW-MASS CLOSE BINARY KIC 9761199

E. Yoldaş[1] and H. A. Dal[1]

Received June 10 2016; accepted November 3 2016

RESUMEN

Presentamos los resultados obtenidos por la Misión Kepler para la variación de la luz de la binaria KIC 9761199. Encontramos que la temperatura de la componente secundaria es de 3891±1 K, el cociente de masas es de 0.69±0.01 y la inclinación orbital es de $77°.4 \pm 0°.1$. Se encontraron manchas estelares separadas entre sí aproximadamente 180° en longitud, a latitudes de +47° y +30°. Se calculó también el modelo OPEA para las 94 ráfagas detectadas. El valor en el plateau fue 1.951±0.069 s, y la vida media fue 1014 segundos. La frecuencia N_1 de las ráfagas fue igual a 0.01351 por hora, mientras que N_2 fue igual a 0.00006. El tiempo máximo de ascenso para las ráfagas fue de 118.098 s, y la duración máxima de éstas fue 6767.72 s. La actividad cromosférica de KIC 9761199 es la que se espera para una $B - V$ de 1.303 mag.

ABSTRACT

We present the results obtained from the analyses of KIC 9761199's light variation acquired by the Kepler Mission. The temperature of the secondary component was found to be 3891±1 K, and the mass ratio was found to be 0.69±0.01 with an orbital inclination of $77°.4 \pm 0°.1$. Stellar spots separated by about 180° longitudinally were found around the latitudes of +47° and +30°. In addition, the OPEA model was derived for 94 detected flares. The plateau value was found to be 1.951±0.069 s, while the half−life value was found to be 1014 s. The flare frequency N_1 was 0.01351 h^{-1}, while the flare frequency N_2 was 0.00006. Maximum flare rise time was 1118.098 s, while maximum flare total time was 6767.72 s. The chromospheric activity level of KIC 9761199 is at the expected level according to a $B - V$ of $1^m.303$.

Key Words: binaries: eclipsing — methods: data analysis — stars: flare — stars: individual (KIC 9761199) — techniques: photometric

1. INTRODUCTION

It has been known for several decades that the population rate of red dwarfs in our Galaxy is about 65%, while seventy-five percent of them show flare activity. The stars exhibiting flare activity are known as UV Ceti type stars (Rodonó 1986). Hence, the population rate of UV Ceti type stars in our Galaxy is about 48.75%, which means that one of every two stars in our galaxy shows the flare phenomenon. As expected, the general population rate of UV Ceti type stars is very high in both open clusters and associations (Mirzoyan 1990; Pigatto 1990). However, the population rate of these stars shows a reducing trend, as the age of the cluster increases according to the Skumanich's law (Skumanich 1972; Pettersen 1991; Stauffer 1991; Marcy & Chen 1992). This is because the mass loss rate is so high due to the flare activity that the evolution tracks of the stars are changed by the mass loss both in their main sequence stages, and also in later stages (Marcy & Chen 1992).

According to recent studies, the mass loss rate of UV Ceti type stars is about $10^{-10} M_\odot$ per year due to flare like events, while the solar mass loss rate is about $2 \times 10^{-14} M_\odot$ per year (Gershberg 2005). The difference between the mass loss ratios is also seen in the flare energy levels of the solar and stellar cases. As it is generally observed in the case of

[1]Department of Astronomy and Space Sciences, University of Ege, Turkey.

RS CVn type active binaries (Haisch et al. 1991), the highest energy detected from the most powerful flares (known as two-ribbon flares) occurring in the Sun was found to be $10^{30} - 10^{31}$ erg (Gershberg 2005; Benz 2008). On the other hand, the flare energy level varies from 10^{28} erg to 10^{34} erg in the case of dMe stars (Haisch et al. 1991; Gershberg 2005), while some stars in young clusters, such as the Pleiades cluster and the Orion association, exhibit powerful flare events, with energies reaching 10^{36} erg (Gershberg & Shakhovskaya 1983).

Although both the mass loss ratios and the flare energy levels are remarkably different between the solar and stellar cases, the flare events occurring in a dMe star are generally explained by the classical theory of solar flares. The main energy source in the flare events is a magnetic reconnection processes (Gershberg 2005; Hudson & Khan 1997). However, this theory does not explain each flare phenomenon observed in UV Ceti type stars. To reach a real solution, all the differences and similarities of the flare events occurring in different types of stars should be examined. Then, it should be identified which parameters such as singularity, binarity, mass, age, ect, cause these differences and similarities. For example, some differences are seen between the flare frequencies from one star to the next. This also occurs for the flare energy spectra.

In this study, we studied out the nature of a low mass eclipsing binary, KIC 9761199, which is different from the classical UV Ceti type stars of spectral type dMe because it is a binary system. We did complete light curve analyses of the system for the first time in the literature in order to find the physical properties of the components, using the PHOEBE V.0.32 software (Prša & Zwitter 2005), whose method depends on the 2003 version of the Wilson-Devinney Code (Wilson & Devinney 1971; Wilson 1990). Then, the out-of-eclipse variations were analyzed, and the flares occurring in the chromospherically active component were detected, allowing us to model the magnetic activity of the system by comparing the active component with its analogue.

KIC 9761199 (KOI 1459) was listed with a B band brightness of $17^m.2$ in the USNO ACT Catalog (Urban et al. 1997) for the first time in the literature. Secondly, KIC 9761199 was listed as J19083435+4630290 in the 2MASS All-Sky Survey Catalogue, where the JHK magnitudes of the system were given as $J = 13^m.574$, $H = 12^m.926$, $K = 12^m.782$ (Kharchenko 2001; Cutri et al. 2003). Although the orbital period of the system (P_{orb}) was determined as 0.692031 day for the first time by Watson (2006), analyzing the data obtained in the Kepler Mission, Coughlin et al. (2011) found that the orbital period of the system (P_{orb}) was 1.3839980 day. There is no detailed light curve analysis of the system, though Borucki et al. (2011) computed the semi-major axis (a) of the system as 0.013 AU, while Coughlin et al. (2011) calculated the inclination (i) of the system as $74^\circ.47$ and noted that there is no third light excess. However, they also noted that the system should be examined performing a complete light curve analysis.

In the Kepler Database, the $(B-V)$ color index of the system is given as $0^m.068$, while the temperature ratio of the components is given as 0.682 by Slawson et al. (2011). In addition, the inclination (i) of the system is listed as $\sin i = 0.99451$. However, this inclination value is not in agreement with $i = 74^\circ.47$ given by Coughlin et al. (2011). According to Walkowicz & Basri (2013), the age of the system is 0.77 Gyr and the $(B-V)$ color index of the system is $1^m.36$.

One of the spectral studies of the system was conduced by Mann et al. (2013). They gave the luminosity (L) of the system as 0.082 $L_\odot$. Using the calibration of some spectral observations, Muirhead et al. (2012) indicated that the system is a binary with components of spectral type of M1, and a distance of about 198 pc. The total masses given in the literature for the components vary from 0.51 $M_\odot$ (Muirhead et al. 2014) to 0.65 $M_\odot$ (Coughlin & López-Morales 2012), while the radii vary from 0.48 $R_\odot$ (Muirhead et al. 2014) to 0.84 $R_\odot$ (Coughlin & López-Morales 2012). The temperatures given in the literature vary from 3742 K (Muirhead et al. 2014) to 4060 K (Coughlin & López-Morales 2012). Using the calibrations, Coughlin & López-Morales (2012) calculated the mass and radius of each component as $M_1 = 0.646 M_\odot$, $M_2 = 0.444 M_\odot$, $R_1 = 0.830 R_\odot$, $R_2 = 0.384 R_\odot$.

2. DATA AND ANALYSES

The Kepler Mission is one of the space missions aimed to find exo-planets. More than 150.000 targets have been already observed (Borucki et al. 2010), (Koch et al. 2010), (Caldwell et al. 2010). The quality and sensitivity of these observations are the highest ever reached in photometry (Jenkins et al. 2010a,b). In these observations, many variable targets such as new eclipsing binaries, etc. have also been discovered (Slawson et al. 2011; Matijevič et al. 2012). There are many single or double

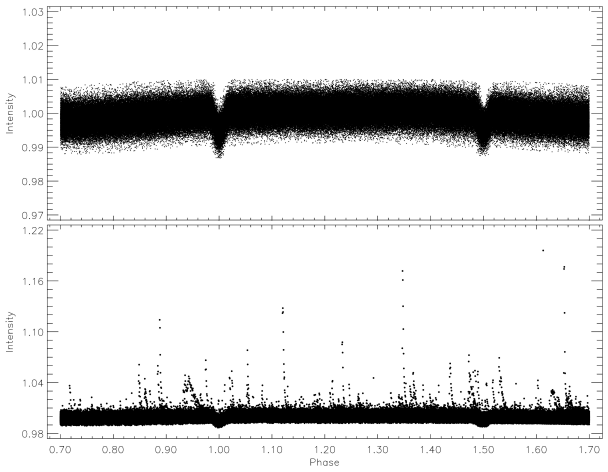

Fig. 1. The light curve of KIC 9761199 obtained from the detrended short cadence data taken from the Kepler Mission database. In the bottom panel, the light curve is plotted with flare activity, while the light curve without flare activity is shown in the upper panel.

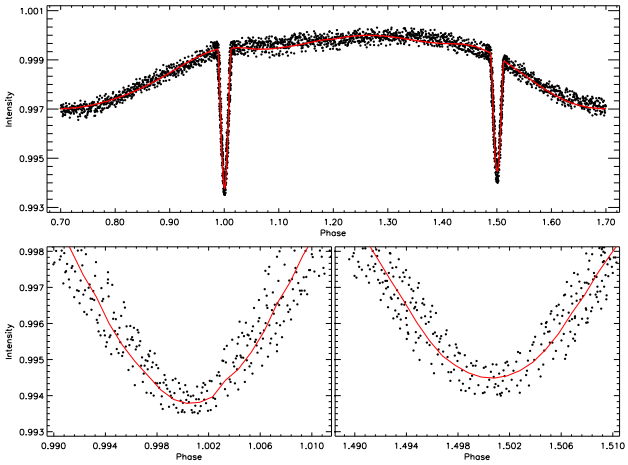

Fig. 2. The observed (filled circles) and synthetic (red smooth line) light curves obtained from the averaged short cadence data acquired from HJD 24 54964.50251 to 24 56424.01145. In the bottom panels of the figure, the minima are plotted in an extended scale, to permit a better view. The color figure can be viewed online.

stars, some of which are eclipsing binaries, exhibiting chromospheric activity (Balona 2015).

The data analyzed in this study were taken from the Kepler Mission Database (Slawson et al. 2011; Matijevič et al. 2012). After removing observations with large errors due to technical problems and using the ephemerides from the Kepler Mission database, the phases were computed. The obtained light curves are shown in Figure 1. Because of the format of this study, the detrended short cadence data were used in the analysis instead of the long cadence. The data were arranged in suitable formats for the analysis of the flare events and the light curve.

2.1. *Light Curve Analysis*

To compute the flare parameters, the synthetic light curve as assumed for the quiescent levels is needed. For this purpose, the light curves shown in the upper panel of Figure 1 were analyzed, after removing the instant-short term light variations due to flare activity. The initial analyses indicated that there are several solutions according to these data. Because of this, the averages of all the detrended short cadence data were computed phase by phase with an interval of 0.001. Then, this averaged light curve shown in Figure 2 was analyzed.

Using the PHOEBE V.0.32 software (Prša & Zwitter 2005), which is included in the 2003 version of the Wilson-Devinney Code (Wilson & Devinney 1971; Wilson 1990), we analyzed the light curves obtained from the averages of all the detrended short cadence data. We attempted to analyze the light curves in various modes, including the detached system mode (Mod2), the semi-detached system mode with the primary component filling its Roche-Lobe mode (Mod4), and the semi-detached system mode with the secondary component filling its Roche-Lobe (Mod5). Our initial analyses demonstrated that an astrophysically reasonable solution was obtainable only in the detached system mode; no results that were statistically consistent with reasonable solutions could be obtained in any of the other modes.

There are several studies about KIC 9761199 in the literature, and many temperature values are given for the system, varying from 3742 K (Muirhead et al. 2014) to 4060 K (Coughlin & López-Morales 2012). To understand which one is right, in this study we calculated both $(H-K)$ and $(J-H)$ color indexes from the JHK magnitudes ($J = 13^m.574$, $H = 12^m.926$, $K = 12^m.782$) given by Kharchenko (2001) and Cutri et al. (2003). Then, using the calibrations of Tokunaga (2000), we derived de-reddened colors as $(H-K)_\circ = 0^m.15$ and $(J-K)_\circ = 0^m.58$. In addition, using the same calibrations, we derived the temperature of the primary component as 4040±20 K, depending on these dereddened colors. In fact, the initial analyses with different temperature values between 3742 K - 4060 K indicated that an astrophysically acceptable solution could be obtained if the temperature was taken as 4060 K for the primary component. Because of this,

TABLE 1

THE PARAMETERS OBTAINED FROM THE LIGHT CURVE ANALYSIS OF KIC 9761199

Parameter	Value
q	0.69±0.01
$i(^\circ)$	77.4±0.1
$T_1(K)$	4060 (fixed)
$T_2(K)$	3891±1
Ω_1	8.96±0.03
Ω_2	7.47±0.03
L_1/L_T	0.61±0.02
g_1, g_2	0.32 (fixed)
A_1, A_2	0.50 (fixed)
$x_{1,bol}$, $x_{2,bol}$	0.696, 0.686 (fixed)
x_1, x_2	0.709, 0.700 (fixed)
$< r_1 >$	0.121±0.001
$< r_2 >$	0.109±0.001
$Co - Lat_{SpotI}$ (rad)	0.82±0.03
$Long_{SpotI}$ (rad)	1.71±0.03
R_{SpotI} (rad)	0.18±0.01
T_{fSpotI}	0.94±0.01
$Co - Lat_{SpotII}$ (rad)	0.52±0.03
$Long_{SpotII}$ (rad)	4.71±0.03
R_{SpotII} (rad)	0.16±0.01
$T_{fSpotII}$	0.95±0.01

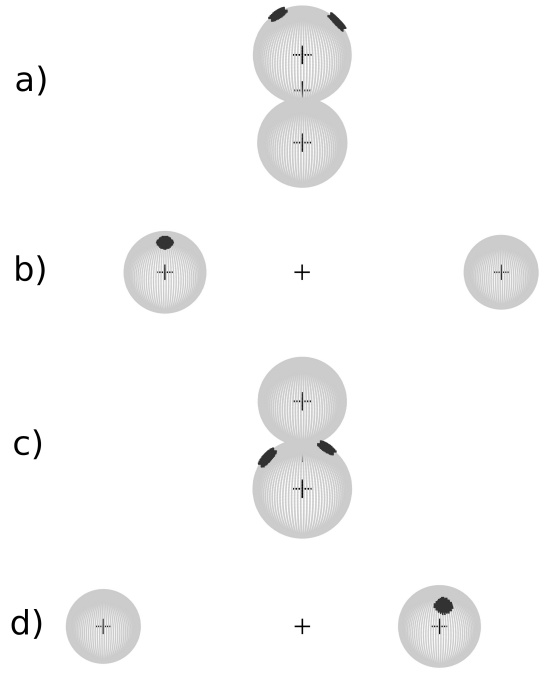

Fig. 3. The 3D model of Roche geometry and the cool spots depending on the parameters obtained from the light curve analysis shown for different phases, such as (a) 0.00, (b) 0.25, (c) 0.50, (d) 0.75.

in the analysis, the temperature of the primary component was fixed at 4060 K, while the temperature of the secondary component was an adjustable parameter. Considering the spectral type corresponding to this temperature, the albedos (A_1 and A_2) and the gravity-darkening coefficients (g_1 and g_2) of the components were adopted for stars with convective envelopes (Lucy 1967; Rucinski 1969). The nonlinear limb-darkening coefficients (x_1 and x_2) of the components were taken from Van Hamme (1993). In the analyses, their dimensionless potentials (Ω_1 and Ω_2), the fractional luminosity (L_1) of the primary component, the inclination (i) of the system, the mass ratio of the system (q), and the semi-major axis (a) were taken as adjustable free parameters.

The out-of-eclipse sinusoidal variation was modelled with two cool spots on the primary component. In the analysis, although the third light was taken as an adjustable free parameter, no third light excess was present in the total light.

All the parameters obtained from the light curve analysis are listed in Table 1. As it can be seen from the table, the error values of each parameter are notably small. This is due to the averaged data used in the analysis. If the original data plotted in the upper panel of Figure 1 were used the error values would be expected to be larger. In addition, apart from some theoretical parameters such as the nonlinear limb-darkening coefficients (x_1 and x_2), the albedos (A_1 and A_2) and the gravity-darkening coefficients (g_1 and g_2), the temperature of the primary component is the only parameter to be fixed in the analysis. However, the temperature of the primary component was not arbitrary assumed. It was determined from the JHK data of system given in the 2MASS All-Sky Survey Catalogue. As a result, the parameters found from the light curve analysis in Table 1 are reliable and can be used to determine the nature of KIC 9761199.

The synthetic light curve obtained with these parameters is shown in Figure 2. In this figure, both primary and secondary minima of the light curve are also plotted in an extended scale, to afford a better view. In addition, the 3D model of the Roche geometry depending on these parameters is shown in Figure 3. The Roche geometry and the cool spot location, depending on the parameters obtained from the

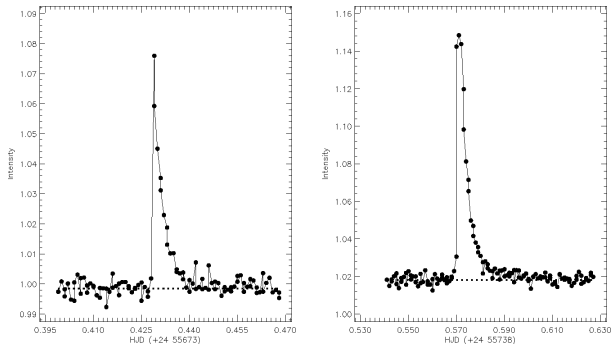

Fig. 4. Two different samples for the flare light variations. In the figure, the filled circles represent the observations, while the dotted lines represent the synthetic light curve obtained by the light curve analysis, which was assumed as the quiescent level for each flare.

light curve analysis, are shown for different phases, namely 0.00, 0.25, 0.50, 0.75.

Although a radial velocity curve is not available, we tried to estimate the absolute parameters of the components, considering the calibrations given by Tokunaga (2000). The $(B-V)$ color index was found to be $1^m.303$ for the primary component depending on the temperature value derived from the analysis. It was $1^m.378$ for the secondary component. These color indexes are in agreement with the value found by Walkowicz & Basri (2013). Using the calibrations given by Tokunaga (2000), the mass of the primary component must be $0.57 \pm 0.01 M_{\odot}$, corresponding to its $(B-V)$ color index. Considering the possible mass ratio of the system, the mass of the secondary component was found to be $0.39 \pm 0.02 M_{\odot}$. Using Kepler's third law, we calculated the possible semi-major axis as $a = 5.16 \pm 0.02 R_{\odot}$. Considering this estimated semi-major axis, the radius of the primary component was computed as $0.62 \pm 0.05 R_{\odot}$, while that of the secondary component was $0.56 \pm 0.05 R_{\odot}$.

2.2. *Flare Activity and the OPEA Model*

To demonstrate the chromospherically active nature of the system, the light variations just due to flare events need to be revealed. For this aim, first all the light variations due to both the geometrical effects and the rotational modulation caused by the spots were removed from the general light variation. For this purpose, the data of all the pre-whitened light curves were obtained. To acquire the pre-whitened data, we extracted the synthetic light curves from all the detrended short cadence data.

In the second step, to determine basic flare parameters such as the first point of the flare onset, the last point of the flare end and the flare energy, the quiescent levels for each flare should be derived. At this point, the synthetic model led us to define the quiescent levels for each flare at the same time. Using the synthetic model as the quiescent level, the parameters of the flares were computed. Two samples of the flare light curves taken from observation data and the quiescent levels derived for these flares are shown in Figure 4.

Using the synthetic models assumed as the quiescent levels, both the beginning and the end of each flare were defined, and then some flare parameters, such as flare rise times (T_r), decay times (T_d), amplitudes of flare maxima, flare equivalent durations (P), were computed. In total, 94 flares were detected from the available short cadence data in the Kepler Mission Database. All the computed parameters are listed in Table 2 for these 94 flares. In the table, flare maximum times, equivalent durations, rise times, decay times and amplitudes of flare maxima are listed in successive columns.

In the analysis, the equivalent durations of the flares were computed using Equation (1) taken from Gershberg et al. (1972):

$$P = \int [(I_{flare} - I_0)/I_0] dt \qquad (1)$$

where I_0 is the flux of the star in the observed band while in quiescent state. In this study, we computed I_0 using the synthetic models derived with the light curve analysis. I_{flare} is the intensity observed at the moment of the flare. P is the flare-equivalent duration in the observed band. In this study, the flare energies (E) were not computed due to the reasons described in detail by Dal & Evren (2010, 2011).

Comparing the relationships of the flare parameters, it is seen that the distributions of flare equivalent durations on a logarithmic scale versus flare total durations vary according to a rule. The distributions of flare equivalent durations on a logarithmic scale cannot be higher than a specific value for the star, no matter how long the flare total duration is. Using the SPSS V17.0 (Green et al. 1999) and GrahpPad Prism V5.02 (Dawson & Trapp 2004) programs, Dal & Evren (2010, 2011) we found that the best function is the One Phase Exponential Association (hereafter OPEA) for the distributions of flare equivalent durations on a logarithmic scale versus flare total durations. The OPEA function has a so-called *Plateau* term, and this makes it a special function in the analyses. The OPEA function is defined by Equation (2):

$$y = y_0 + (Plateau - y_0) \times (1 - e^{-k \times x}) \qquad (2)$$

TABLE 2

FLARE PARAMETERS COMPUTED FOR THE SHORT CADENCE DATA OF KIC 9761199 AVAILABLE IN THE KEPLER MISSION DATABASE

Flare Time (+24 00000)	P (s)	T_r (s)	T_d (s)	Amplitude (Intensity)
55648.62149	10.66427	294.25248	882.75744	0.03506
55654.62302	3.46467	117.70704	411.95088	0.01650
55656.57790	2.75499	58.84877	470.80915	0.01424
55657.21749	4.84865	117.69840	411.95952	0.02263
55668.99378	6.77842	117.69840	411.95261	0.03122
55671.88592	5.40725	235.39594	470.81088	0.02135
55673.42871	21.66523	58.85741	1000.46189	0.07746
55682.84894	23.99511	353.10384	1824.38525	0.02916
55690.01663	7.87550	176.55667	823.90608	0.02173
55690.40829	3.41761	176.55667	235.39680	0.01292
55691.66023	2.52343	176.54717	176.55667	0.01662
55691.88910	2.80804	58.75200	294.62400	0.01503
55693.20098	8.51286	235.41408	706.20768	0.02361
55694.47881	13.31688	353.10384	823.92336	0.02229
55694.63820	2.09756	176.55581	235.40544	0.01227
55696.43438	6.47066	353.11248	588.51706	0.01321
55697.18023	15.54061	353.10384	823.90522	0.04237
55698.16517	4.10949	117.69840	470.81002	0.01660
55701.69145	30.56748	411.96125	2412.88330	0.03340
55710.67574	11.65687	176.53853	1059.31757	0.02503
55710.97272	4.24631	176.55581	294.25421	0.02309
55716.28700	18.88827	294.25334	1412.41018	0.04641
55719.31808	10.14314	176.55494	882.76003	0.02788
55722.99896	11.08245	235.39507	823.91818	0.03130
55724.14396	9.62495	176.54630	1118.16202	0.02696
55724.95043	4.94587	117.68890	411.96816	0.01795
55728.06529	56.09567	235.39507	2059.76563	0.07023
55730.64953	13.13169	176.54544	1059.31066	0.02468
55731.55544	2.16425	117.68890	117.70618	0.01401
55733.11593	3.79166	117.69754	235.40285	0.02496
55733.13705	1.92040	235.39421	117.70618	0.01899
55733.40201	12.70762	117.69754	941.60362	0.03861
55738.40292	12.15108	176.55408	1059.30720	0.02349
55738.57116	58.17733	294.25939	2471.71478	0.13029
55740.56212	11.68516	176.54544	1412.40586	0.02275
55744.06656	2.99633	235.40198	235.40198	0.01388
55744.08495	1.73474	117.68803	117.70531	0.01503
55754.92383	130.99219	647.35459	6120.36691	0.04921
55772.29873	19.12241	235.40717	823.88189	0.05312
55773.26593	1.58905	58.84704	294.25421	0.01069
55774.78756	2.74595	176.55062	235.38989	0.01329
55775.25413	6.79622	58.85568	706.17744	0.02373
55775.61308	30.78613	176.55062	2059.71811	0.06187
55783.59719	80.32655	235.38816	2942.44013	0.17808
55785.26730	12.48313	117.69408	647.34250	0.04444
55785.57517	16.66883	176.54112	1530.07402	0.03594
55787.04434	2.90663	235.38816	235.40458	0.01604
55788.38615	5.19716	117.69322	588.49546	0.01873
55788.73897	17.18207	176.53162	1471.22438	0.03291
55791.99062	15.28898	117.69408	1000.42128	0.03837
55795.39620	2.86915	117.70186	176.54890	0.01564
55819.27527	45.55776	706.16794	2589.28704	0.06316

TABLE 2. CONTINUED

Flare Time (+24 00000)	P (s)	T_r (s)	T_d (s)	Amplitude (Intensity)
55796.34364	3.53016	58.85482	470.78237	0.01915
55801.73670	5.81090	176.54803	411.93360	0.02571
55804.52926	2.98768	117.70099	294.24038	0.01691
55820.37526	14.11267	353.08310	1353.48883	0.01976
55805.77229	68.48297	235.38557	6120.19670	0.02991
55806.37235	4.65150	235.38557	588.47990	0.01775
55809.49865	46.23526	882.71856	1235.79562	0.05201
55810.42632	4.35491	235.38470	353.08570	0.01401
55813.21546	17.71834	176.53853	1412.35747	0.03683
55814.02734	4.33411	58.85395	353.07619	0.02484
55815.19204	6.06366	58.85482	823.86115	0.01632
55815.65178	3.20557	58.85482	411.93014	0.01947
55825.57891	6.81791	176.53680	588.47386	0.02193
55828.40004	24.12872	176.55408	1588.86576	0.05481
55832.00784	67.89115	1118.09894	4413.55046	0.03464
55842.95719	3.41716	58.85395	353.07187	0.01880
55846.62150	7.68861	117.69840	588.47731	0.02595
55848.41960	5.73742	117.68976	529.63200	0.02068
55852.56067	20.40242	353.08829	1235.78006	0.05653
55862.50127	31.43598	647.31053	1765.39910	0.03707
55874.87472	17.49964	176.52557	1118.09462	0.04550
55878.24750	3.98561	176.54285	411.92237	0.01816
55880.92556	26.30278	176.53421	1412.32723	0.06571
55881.21230	4.94509	176.53421	411.93965	0.02558
55881.32536	9.92092	176.53507	823.85251	0.02456
55884.23091	6.25840	235.37952	765.00806	0.01940
55886.83678	10.71779	58.84445	823.85338	0.03534
55886.96755	22.22971	294.24125	1647.69811	0.02492
55888.44757	6.25139	117.69840	588.45658	0.02182
55891.30271	73.14961	470.77546	2883.48422	0.07367
55896.11193	7.12551	117.69840	706.15584	0.02458
55911.04562	4.48567	235.38038	294.24298	0.02266
55913.35318	4.19466	117.69840	294.22570	0.01940
55913.69850	16.36581	353.07965	1412.31946	0.02380
55918.65009	31.09451	117.69926	1294.63142	0.08420
55919.97075	6.28820	176.53594	588.47990	0.01913
55920.43049	30.97705	411.92669	1647.71280	0.04837
55921.79746	16.13419	176.54458	765.00720	0.04360
55921.93640	5.16064	235.38125	411.94397	0.02153
55922.14755	4.60511	176.53680	647.32522	0.01316
55925.62593	4.94213	176.54544	470.77286	0.02649
55929.51435	8.85268	117.70013	823.85597	0.02607

where the parameter y is the flare equivalent duration on a logarithmic scale, the parameter x is the flare total duration, according to the definition of Dal & Evren (2010), and the parameter y_0 is the flare-equivalent duration in on a logarithmic scale for the least total duration. In other words, the parameter y_0 is the least equivalent duration occurring in a flare for a star. An important point here is that the parameter y_0 does not depend only on the flare mechanism occurring in the star, but also on the sensitivity of the optical system used for the observations. The parameter *Plateau* value is the upper limit for the flare equivalent duration on a logarithmic scale. Dal & Evren (2011) defined the *Plateau* value as a saturation level for a star in the observed band.

Using the least-squares method, the OPEA model was derived for the distributions of flare equivalent durations on a logarithmic scale versus flare total durations. The derived model is shown in Fig-

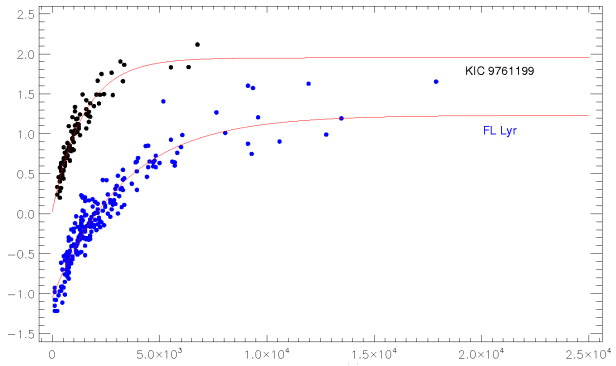

Fig. 5. The OPEA model derived from 94 flares detected in the available short cadence data of KIC 9761199 in the Kepler Mission Database is shown, compared to the OPEA model obtained from the data of the well known eclipsing binary, FL Lyr (Yoldaş & Dal 2016). In the figure, the filled circles represent the calculated log(P) values from the observations, while the lines represent the OPEA models.

ure 5 together with the observed flare equivalent durations, while the parameters computed from the model are listed in Table 3. The *span* value listed in the table is the difference between the *Plateau* and y_0 values. According to the definition of the OPEA function, the parameter k in Equation (2) is a constant for just this model, depending on the x values. The half−life value is half of the first x value, at which the model reaches the *Plateau* value. In other words, it is half of the minimum flare total time, which is enough to provide the maximum flare energy occurring in the flare mechanism.

The model was tested by using three different methods, such as the D'Agostino-Pearson normality test, the Shapiro-Wilk normality test and also the Kolmogorov-Smirnov test, given by D'Agostino & Stephens (1986), to understand whether there are any other functions to model the distributions of flare equivalent durations on a logarithmic scale versus flare total durations. In these tests, the probability value called $p-$value was found to be < 0.001 and this means that there is no other plausible function to model the distributions of flare equivalent durations (Motulsky 2007; Spanier & Oldham 1987).

KIC 9761199 was observed for as long as 289.82931 days from JD 2455641.50631 to JD 2455931.33562 without any remarkable interruptions. In total, 94 significant flares were detected in these observations. The total flare equivalent duration computed from all the flares was found to be 628.11671 s (0.17448 hours). Ishida et al. (1991) described two frequencies for the stellar flare activity. These frequencies are defined by Equations (3) and (4):

$$N_1 = \Sigma n_f \; / \; \Sigma T_t \tag{3}$$

$$N_2 = \Sigma P \; / \; \Sigma T_t \tag{4}$$

where Σn_f is the total flare number detected in the observations, and ΣT_t is the total observing duration, while ΣP is the total equivalent duration obtained from all the flares. In this study, the N_1 frequency was found to be 0.01351 h^{-1}, and the N_2 frequency was 0.00006.

3. RESULTS AND DISCUSSION

The results obtained from the analyses of short cadence data in the Kepler Mission Database indicate that KIC 9761199 exhibits high level chromospheric activity. However, it is necessary to identify which component is active. Then, it should be compared with its analogue to be certain about the activity level of the system. All these data are needed to determine the physical parameters of the components.

Although all the variations apart from the geometrical effect, such as flare activity, were removed from the short cadence data taken from the database, neither the eclipses nor any other variation could be seen clearly in the eliminated data, as shown in the upper panel of Figure 1. For the light curve analysis, we computed the averages phase by phase with an interval of 0.001 for the eliminated short cadence data. As shown in Figure 2, both the primary and secondary minima, and also a sinusoidal variation due to the rotational modulation, are clearly visible in these averaged data. An important point is that the amplitude difference between the primary and secondary minima can be visible. This is important because the orbital period of the system is controversial in the literature (Watson 2006; Coughlin et al. 2011). However, this figure demonstrates that the orbital period of the system is 1.3839980 day, not 0.692031 day. According to this result, first of all, KIC 9761199 is a double object. There are two different minima, and the secondary object cannot be a planet: it must be a star. If it were a planet, there would not be any secondary minimum in the light curve due to the contrast effect between a star and a planet.

Although there are a few approaches using calibrations for the physical parameters of the components, there is no complete light curve analysis for

TABLE 3

THE OPEA MODEL PARAMETERS BY USING THE LEAST-SQUARES METHOD

Parameter	Values	95% Confidence Intervals
Y_0	0.027±0.054	−0.081 to 0.135
$Plateau$	1.951±0.069	1.813 to 2.089
K	0.0007±0.0001	0.0006 to 0.0008
Tau	1462.9	1232.6 to 1799.1
Half−life	1014	854.4 to 1247.1
Span	1.924±0.062	1.800 to 2.048
Goodness of Fit	Method	Values
R^2		0.9186
$p-$value	(D'Agostino-Pearson)	0.0011
$p-$value	(Shapiro-Wilk)	0.0009
$p-$value	(Kolmogorov Smirnov)	0.0009

KIC 9761199 in the literature. For this purpose, the light curve obtained from the detrended short cadence data was analyzed, using the PHOEBE V.0.32 software (Prša & Zwitter 2005), which is employed in the 2003 version of the Wilson-Devinney Code (Wilson & Devinney 1971; Wilson 1990). Although the spectral type was given as M1 V for KIC 9761199 (Muirhead et al. 2012), there are several temperature values mentioned for this system. According to the de-reddened colors $(H-K)_\circ = 0^m.15$ and $(J-K)_\circ = 0^m.58$ of the system, the temperature of the primary component was taken to be 4060 K as given by Coughlin & López-Morales (2012). In the light curve analysis with the PHOEBE V.0.32 software, the temperature of the secondary component was found to be 3891±1 K. The mass ratio of the system (q) was found to be 0.69±0.01, while the inclination (i) of the system was $77^\circ.44 \pm 0^\circ.01$.

In addition, as shown in Figure 1 and in the upper panel of Figure 2, the light curve exhibits a remarkable sinusoidal variation at out-of-eclipse. This variation could be caused by the effects of tidal distortion, or by the mutual heating of the components themselves. All these cases were included to the analysis. For this aim, the albedos (A_1 and A_2), and the gravity-darkening coefficients (g_1 and g_2) of the components were computed depending on their temperatures; their dimensionless potentials (Ω_1 and Ω_2) were also derived in the analysis. However, the initial results showed that the synthetic light curve obtained with these parameters did not fit the observations. At this point, considering both the temperatures and the fractional radii of the components, and also the flare activity, we assumed that this sinusoidal variation was caused by the rotational modulation due to the stellar cool spots. Because of this, the sinusoidal variation was modelled with two cool spots on the primary component. The spots were separated by about 180° longitudinally, while one of them was located at about latitude $47^\circ.0 \pm 0^\circ.2$ and the other one was located at about latitude $30^\circ.0 \pm 0^\circ.2$. The cool spots were assumed to be located on the primary component. However, they could likely be located on the secondary component, and this could also provide an acceptable solution, astrophysically. A strong clue for the answer of this quandary is given by the discussion of flare activity in the latter part of the text. The 3D model of the Roche geometry for the components and the cool spots on the primary component is shown in Figure 3 for different phases.

Considering both the component temperatures and the fractional radii found from the light curve analysis, and using the calibrations given by Tokunaga (2000), and also Kepler's third law, we tried to estimate the absolute parameters of the components. The mass of the primary component was found to be $0.57 \pm 0.01 M_\odot$, that of the secondary $0.39 \pm 0.02 M_\odot$. In addition, the radius of the primary component was computed as $0.62 \pm 0.05 R_\odot$, while that of the secondary component was $0.56 \pm 0.05 R_\odot$.

Considering the results of the analysis, it is seen that both locations of the stellar spots are not changed on the primary component along 289.82931 days (9.66 months), that is, along the whole observing season. However, a spotted area evolves in 2 to 3 months at most in the solar case (Gershberg 2005). On the other hand, according to Hall et al. (1989) and Gershberg (2005), it is well known that the spotted areas on the active compo-

nents of some RS CVn binaries, such as V478 Lyr, can keep their shapes and locations for about two years. Therefore, the behaviour of the cool spot activity observed in the case of KIC 9761199 is not inconsistent with the stellar spot activity phenomenon. It must be noted that although we used the word spot, we actually refer to an active area, in which several spots can appear and disappear in time. Here, the question to be answered is why the locations of these areas are stable for 289.82931 days. This is a discussion about the differential rotation of the components.

We detected 94 flare events in KIC 9761199, and calculated some parameters for each flare, such as flare frequencies. Yoldaş & Dal (2016) recently resolved the nature of the chromospheric activity of a different system, FL Lyr. They found flare frequencies of $N_1 = 0.41632h^{-1}$ and $N_2 = 0.00027$ for that system. Comparing the flare frequencies of KIC 9761199 with those of FL Lyr, it is clearly seen that FL Lyr exhibits flares more frequently than KIC 9761199, and also that its flares are more powerful than those of KIC 9761199. Comparing KIC 9761199's flare frequency values with those found for UV Ceti type flare stars for spectral types dK5e to dM6e, the flare energies obtained for KIC 9761199 are remarkably lower than those of UV Ceti stars. For instance, the observed flare number per hour for AD Leo was found to be $N_1 = 1.331h^{-1}$, while $N_1 = 1.056h^{-1}$ for EV Lac. Moreover, the N_2 frequency was 0.088 for EQ Peg, $N_2 = 0.086$ for AD Leo (Dal & Evren 2011). As it is clearly seen from these results, the flare frequencies of KIC 9761199 are remarkably small. However, it is well known (Dal & Evren 2011) that the flare frequency can dramatically change from one season to the next for some stars, such as V1005 Ori, EV Lac, etc. In this case, there could be some changes in the flare frequency and the flare behaviour of KIC 9761199 in the next observing seasons. In addition, the results found from the flare frequency analyses reveal why no flare had been detected for this system by ground based telescopes before the Kepler Mission. If the N_2 frequency is considered, it will be understandable, because N_2 indicates that the flare events occurring on the active component of the system are too weak to be observed by ground based telescopes.

The *Plateau* value was found to be 1.951 ± 0.069 s from the OPEA model, derived from the variation of the flare equivalent duration distributions on a logarithmic scale versus flare total durations for 94 flares. However, Yoldaş & Dal (2016) found the *Plateau* value as 1.232 ± 0.069 s for FL Lyr. Moreover, Dal & Evren (2011) computed the *Plateau* values for some UV Ceti type stars. They gave the *Plateau* values as 3.014 s for EV Lac ($B - V = 1^m.554$), 2.935 s for EQ Peg ($B - V = 1^m.574$), and 2.637 s for V1005 Ori ($B-V = 1^m.307$). Clearly, the maximum flare energy detected for KIC 9761199 is remarkably smaller than the maximum energy level obtained for UV Ceti type single flare stars. The *Plateau* value of this system approaches the value obtained from V1005 Ori. It must be noted that Dal & Evren (2011) found that the *Plateau* value is always constant for a star, but it changes from one star to the other depending on their $B - V$ color indexes. Dal & Evren (2011) defined the *Plateau* value as the energy saturation level for the flare mechanism occurring in the star. As a result, the flare activity should have occurred on the primary component given its $B - V$ color index. If it had ocurred on the secondary component, the *Plateau* value of KIC 9761199 would be incompatible according to the analogue of the secondary component.

Using the regression calculations, the half−life value was found to be 1014.0 s from the OPEA model for KIC 9761199. In the case of FL Lyr, it was 2291.7 s (Yoldaş & Dal 2016). This means that a flare occurring on the FL Lyr can reach the maximum energy level when the flare total duration reaches $n \times 38$ minutes, while it takes $n \times 17$ minutes for KIC 9761199. Here n is a constant depending on the OPEA function of a star (Spanier & Oldham 1987; Dawson & Trapp 2004; Motulsky 2007). In other words, the parameter half−life refers to a minimum duration limit for a flare to reach maximum energy. In this perspective, the flares, whose total times are shorter than $n \times 17$ minutes, can never reach the *Plateau* value obtained from the OPEA model derived for the flares of KIC 9761199. This value is a few times larger than those obtained for single dMe stars. For single dMe stars, for example, it was found to be 433.10 s for DO Cep ($B-V = 1^m.604$), and 334.30 s for EQ Peg, while it is 226.30 s for V1005 Ori (Dal & Evren 2011). This means that for stars such as EQ Peg, V1005 Ori and DO Cep, the flares can reach the maximum energy level at their *Plateau* value, when their total durations reach about $n \times 5$ minutes, while they need $n \times 17$ minutes for KIC 9761199.

On the other hand, the maximum flare rise time (T_r) obtained for the flares of the eclipsing binary KIC 9761199 was found to be 1118.098 s, while (T_t) was 6767.72 s. However, these values are

$T_r = 5179.00$ s and $T_t = 12770.62$ s for FL Lyr. As a result, the FL Lyr flare time scales are larger than those obtained from KIC 9761199, which is in agreement with the results found by Dal & Evren (2011) for single dMe flare stars. In the light curve analysis, the primary component was assumed to be the chromospherically active component and its color index was $(B-V) = 1^m.303$. However, the $(B-V)$ color index of the active component of FL Lyr is $0^m.74$. Consequently, the chromospherically active component of KIC 9761199 is cooler than that of FL Lyr. In this case, the flare time scales of FL Lyr must be larger, according to Dal & Evren (2011).

Finally considering the *Plateau* value, the flare frequencies and the flare time scales, it is clear that the flare activity level of KIC 9761199 is lower than that of almost all the UV Ceti type stars, as for instance FL Lyr. This result about the chromospheric activity level of the system is also in agreement with Dal & Evren (2011). The authors indicated that the parameters derived from the OPEA model of a star depend on just the $(B-V)$ color index of that star. In other words, the OPEA model parameters increase or decrease according to the variation of the $(B-V)$ color index. As a matter of course, the OPEA model parameters derived for KIC 9761199 were found to be closer to the expected values for the $(B-V)$ color index of the primary component, not to that of the secondary component.

To recapitulate: comparing the flare activity of KIC 9761199 indicated that the assumption that "the chromospherically active star was the primary component of the system" is correct. In addition, the statistical analyses of the OPEA model demonstrated that there was only one star exhibiting flare activity in the system. According to the statistical analyses, the probability value was found to be $p - value < 0.001$. This means that there is no other plausible function to model the distributions of flare equivalent durations (Motulsky 2007; Spanier & Oldham 1987). Therefore, there is only one star exhibiting flare activity.Considering the classical theory of solar flares (Gershberg 2005), the star exhibiting flare activity and cool spot activity must be the same star.

According to Dal & Evren (2011), it is a contentious issue which parameter, the *Plateau* value or the flare frequencies (N_i), is the best indicator for the activity level. In general, the chromospheric activity level of a system depends on several parameters, especially on the stellar rotation velocity. The rotation velocity depends on the stellar age or on its being a component of a close binary. Because of this, we discussed KIC 9761199 for both cases. Firstly, the age of KIC 9761199 is given as 0.77 Gyr (Walkowicz & Basri 2013), while the age of FL Lyr is between 3.05 Gyr and 15.25 Gyr according to the literature. Considering Skumanich (1972)'s law, the activity level of KIC 9761199 would be expected to be clearly higher than that of FL Lyr. Secondly, in this study we computed the radii of the components as $R_1 = 0.62R_\odot$ and $R_2 = 0.56R_\odot$, and the semi-major axis as $5.16R_\odot$. However, the radii of the FL Lyr components are $R_1 = 1.283R_\odot$, $R_2 = 0.963R_\odot$, and its semi-major axis $a = 9.17R_\odot$ (Eker et al. 2014). According to these absolute parameters, the activity level of KIC 9761199 should be higher than that of FL Lyr. Also, the flare frequencies (N_i) of FL Lyr are higher than those of KIC 9761199. However, the *Plateau* value of KIC 9761199 is clearly higher than that of FL Lyr. According to the semi-major axis of the KIC 9761199, the components are closer to each other than those of FL Lyr. Maybe this is why the *Plateau* value is higher in the case of KIC 9761199. However, this is still an unsolved point. Why are the flare frequencies higher in the case of FL Lyr? A similar phenomenon is also common among the UV Ceti type single stars (Dal & Evren 2010, 2011).

As a result, according to the possible masses and radii of the components, KIC 9761199 must be a low-mass, close binary system. In addition, according to the OPEA model parameters, just one component of the system is chromospherically active. Both the age given in the literature and the proximity of the components can help to keep the activity level high. However, the active component exhibits intense flare activity, but quiescent spot activity. This does not mean that the cool spot activity level is low in this system. It is possible that the active component could be covered by some large spots spread over its surface. In this case, there would be no rapid light variation in the out-of-eclipse light curve contrary to the case of FL Lyr. To reveal and understand the nature of the cool spot activity in this system, it is necessary to track the sinusoidal light variation due to the rotational modulation in the light curve. However, these observations will be very difficult for ground based telescopes due to sensitivity problems. In addition, there is no detailed spectroscopic observation of KIC 9761199 in the literature. This is also needed for future studies.

The authors thank the referee for useful comments that contributed to the improvement of the paper.

REFERENCES

Balona, L. A. 2015, MNRAS, 447, 2714

Benz, A. O. 2008, Living Rev. Solar Phys., 5, 1

Borucki, Wi. J., Koch, D. G., Basri, G., et al. 2010, Sci, 327, 977

Borucki, Wi. J., Koch, D. G., Basri, G., et al. 2011, ApJ, 736, 19

Caldwell, D. A., Kolodziejczak, J. J., & Van Cleve, J. E. 2010, ApJL, 713, L92

Coughlin, J. L., López-Morales, M., Harrison, T. E., et al. 2011, AJ, 141, 78

Coughlin, J. L. & López-Morales, M. 2012, AJ, 143, 39

Cutri, R. M., Skrutskie, M. F., van Dyk, S., et al. 2003. The IRSA 2MASS all sky point source catalog. NASA IPAC Infrared Science Archive `http://irsa.ipac.caltech.edu/applications/Gator`

D'Agostino, R. B. & Stephens, M. A. 1986, Tests for Normal Distribution in Goodness-Of-Fit Techniques, Statistics: Textbooks and Monographs, New York: Dekker, edited by D'Agostino, R. B. & Stephens, M. A.

Dal, H. A. & Evren, S. 2010, AJ, 140, 483

_____. 2011, AJ, 141, 33

Dal, H. A., Sipahi, E., & Özdarcan, O. 2012, PASA, 29, 150

Dawson, B. & Trapp, R. G. 2004, Basic and Clinical Biostatistics (New York: McGraw-Hill), 61

Eker, Z., Bilir, S., Soydugan, F., et al. 2014, PASA, 31, 24

Gershberg, R. E. & Shakhovskaya, N. I. 1983, Astrophys. Space Sci., 95, 235

Gershberg, R. E. 1972, Astrophys. Space Sci., 19, 75

_____. 2005, Solar-Type Activity in Main-Secauence Stars, Springer Berlin Heidelberg, New York, 53, 191, 360

Green, S. B., Salkind, N. J., & Akey, T.M. 1999, Using SPSS for Windows: Analyzing and Understanding Data (Upper Saddle River, NJ: Prentice Hall), 50

Haisch, B., Strong, K. T., & Rodonó, M. 1991, ARA&A, 29, 275

Hall D. S., Henry G. W., & Sowell J. R. 1989. AJ, 99, 396

Hudson, H. S. & Khan, J. I. 1997, in ASP Conf. Ser. 111, Magnetic Reconnection in the Solar Atmosphere, ed. R. D. Bentley & J. T. Mariska (San Francisco, CA: ASP), 135

Ishida, K., Ichimura, K., Shimizu, Y., et al. 1991, Ap&SS, 182, 227

Jenkins, J. M., Caldwell, D. A., Chandrasekaran, H., et al. 2010a, ApJL, 713, L87

Jenkins, J. M., Chandrasekaran, H., McCauliff, S. D., et al. 2010b, Proc. SPIE, 7740, 77400

Kharchenko, N. V. 2001, KFNT, 17, 409

Koch, D. G., Borucki, W. J., Basri, G., et al. 2010, ApJL, 713, L79

Lucy, L. B. 1967, Z. Astrophys, 65, 89

Mann, A. W., Gaidos, E., & Ansdell, M. 2013, ApJ, 779, 188

Marcy, G. W. & Chen, G. H. 1992, ApJ, 390, 550

Matijevič, G., Prša, A., Orosz, J. A., et al. 2012, AJ, 143, 123

Mirzoyan, L. V. 1990, in IAU Symp. 137, Flare stars in star clusters, associations and the solar vicinity, proceedings of the 137th IAU Symposium, Byurakan, Armenian SSR, Oct. 23-27, 1989 (A91-55760 24-90). Dordrecht, Netherlands, Kluwer Academic Publishers, 1990, 1

Motulsky, H. 2007, in GraphPad Prism 5: Statistics Guide, San Diego, CA: GraphPad Software Inc. Press, 94

Muirhead, P. S., Becker, J., Feiden, G. A., et al. 2014, ApJS, 213, 5

Muirhead, P. S., Hamren, K., Schlawin, E., et al. 2012, ApJL, 750, 37

Pettersen, B. R. 1991, Mem. Soc. Astron. Ital., 62, 217

Pigatto, L. 1990, in IAU Symp. 137, Flare stars in star clusters, associations and the solar vicinity, proceedings of the 137th IAU Symposium, Byurakan, Armenian SSR, Oct. 23-27, 1989 (A91-55760 24-90). Dordrecht, Netherlands, Kluwer Academic Publishers, 1990, 117

Prša, A. & Zwitter, T. 2005, ApJ, 628, 426

Rodonó, M. 1986, NASSP, 492, 409

Rucinski, S. M. 1969, AcA, 19, 245

Skumanich, A. 1972, ApJ 171, 565

Slawson, R., Prša, A., Welsh, W.F., et al. 2011, AJ, 142, 160

Spanier, J. & Oldham, K. B. 1987, in An Atlas of Function, Washington, DC: Hemisphere Publishing Corporation Press, 233

Stauffer, J. R. 1991, in Proc. NATO Advanced Research Workshop on Angular Momentum Evolution of Young Stars, ed. S. Catalano & J.R. Stauffer (Dordrecht: Kluwer), 117

Tokunaga, A. T. 2000, in Allen's Astrophysical Quantities, ed. A.N. Cox (Springer), 143

Urban, S., Corbin, T., & Wycoff, G. 1997, AAS, 191, 5707

Van Hamme, W. 1993, AJ, 106, 2096

Walkowicz, L. M. & Basri, G. S. 2013, MNRAS, 436, 1883

Watson, C. L. 2006, SASS, 25, 47

Wilson, R. E. 1990, ApJ, 356, 613

Wilson, R. E. & Devinney, E. J. 1971, ApJ, 166, 605

Yoldaş, E. & Dal, H. A. 2016, PASA, 33, 16

E. Yoldaş & H. A. Dal: Department of Astronomy and Space Sciences, University of Ege, Bornova, 35100 İzmir, Turkey (ezgiyoldas@gmail.com, ali.dal@ege.edu.tr).